

Interaction Notes

Note 408

July 1981

DETERMINATION OF SEM POLES FROM FREQUENCY RESPONSES

J. M. Pond and T.B.A. Senior
Radiation Laboratory
Department of Electrical and Computer Engineering
The University of Michigan
Ann Arbor, Michigan 48109

Abstract

A curve fitting and pole extraction algorithm has been developed and applied to exact frequency domain data for the surface fields on a perfectly conducting sphere. The data are fitted extremely close and for at least a handful of the lowest order SEM poles, the extracted poles and their residues are in good agreement with their known exact values. Unfortunately, this is not true if the frequency response is degraded in accuracy. In particular, noise effects are explored, and it is found that for noise levels typical of the best experimental data, it is no longer possible to locate more than (at most) the dominant SEM pole to a reasonable degree of accuracy.

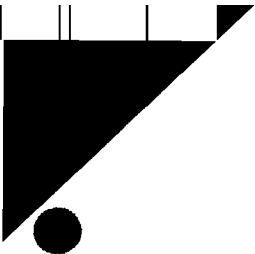
DETERMINATION OF SEM POLES FROM FREQUENCY RESPONSES

1. Introduction

The singularity expansion method (SEM) is based on the analytic properties of the electromagnetic response of a body as a function of the complex frequency s . For a passive body the singularities are confined to the left half of the complex s plane, and a knowledge of these singularities can serve to characterize the response to any excitation. If the body is finite and perfectly conducting, the only singularities in the finite part of the plane are poles, which are simple and occur in complex conjugate pairs (Baum, 1976; Sancer and Varvatsis, 1980), i.e., are symmetrically placed with respect to the negative real s axis.

It is fundamental to SEM that the poles are independent of the mathematical representation of the response and are a property of the body alone. In particular, their locations (but not the residues) are unaffected by a change in the illumination, and if a collection of poles is extracted from computed or measured data for the response, the SEM poles can be distinguished from numerical artifacts by their positional invariance. Cataloging the true poles is therefore a simple method of summarizing information about a body, and their extraction from measured data could serve as a means of target identification.

Several numerical algorithms exist for determining the SEM poles from frequency domain data. One of these is an iterative method developed by Sharpe and Roussi (1979) and based on a technique of Levy (1959). It



is essentially a least squares method that fits the data with a rational function from which the poles and residues are then computed. The iteration linearizes the calculation and also reduces the excessive weighting of the higher frequencies that a straight least squares computation normally produces. The program was initially applied to measured data for the axial current at several locations on a thick cylinder over a frequency range spanning the first five longitudinal modes. In every instance the rational function obtained gave an excellent fit to the measured data curve, but apart from the lowest order one, the poles were not positionally invariant. As the angle of illumination changed, all poles except the first showed substantial movement in the complex plane, and it proved impossible to achieve a fit when the movement was restricted. Of course, for a thick cylinder the SEM poles are not known precisely.

The extent to which the lack of success was due to the program itself, the selection of such parameters as the sampling interval and the order of the rational function, or to the noise and other inaccuracies in the measured data, was not apparent. In the time domain it is found (Cho and Cordaro, 1980) that pole extraction is quite sensitive to noise. To see if this same sensitivity exists in the frequency domain and, at the same time, gain experience in the application of the program, it is helpful to consider data whose accuracy can be controlled. The only finite body whose frequency response is easily obtained to any accuracy desired is the sphere, and in the following sections we consider the determination of the poles and residues from frequency domain data for the surface fields on a

perfectly conducting sphere. For this body the SEM poles and residues are known precisely. After a brief description of the numerical algorithm and the computation of the exact surface fields, poles and residues (Section 2), the extraction of the poles and residues from the frequency response data is discussed (Section 3), along with the influence of the various parameters in the algorithm. In Section 4 we then consider the effect of noise and other data inaccuracies on the pole extraction process.

2. Formulation

Over any finite frequency range the electromagnetic response of a body can be approximated by a rational function whose poles can be found. It is assumed that a subset of these approximate the SEM poles which are dominant in this frequency range and can be distinguished by their positional invariance to a change in excitation of the body. It follows that the most effective pole extraction procedure is one that accurately determines the SEM poles and maximizes the subset.

Given a (complex) frequency response $F(\omega_\ell)$ where $\omega_\ell, \ell = 1, 2, \dots, L$, are sampled (real) frequencies, the numerical algorithm employed fits this with a rational function

$$\frac{N(\omega)}{D(\omega)} = \frac{a_0 + a_1 \omega + \dots + a_m \omega^m}{b_0 + b_1 \omega + \dots + b_n \omega^n} \quad (m \leq n) \quad . \quad (1)$$

The initial curve fit is obtained when the error

$$E = \sum_{\ell=1}^L \left| D(\omega_\ell) F(\omega_\ell) - N(\omega_\ell) \right|^2$$

is minimized, subject to the constraint $b_0 = 1.0$ by solving the simultaneous set of equations

$$\frac{\partial E}{\partial a_j} = 0, \quad j = 0, 1, \dots, m$$

$$\frac{\partial E}{\partial b_j} = 0, \quad j = 1, 2, \dots, n$$

for the coefficients a_j and b_j . The square of the resulting denominator is then used as a weighting factor in a further application of least squares to improve the rational function fit, giving rise to an iterative procedure. At the k th stage of iteration, the coefficients are obtained by minimizing

$$E = \sum_{\ell=1}^L \left| \left\{ D_k(\omega_\ell) F(\omega_\ell) - N_k(\omega_\ell) \right\} \left\{ D_{k-1}(\omega_\ell) \right\}^{-1} \right|^2, \quad (2)$$

and so on until the error is less than a pre-specified value.

A program has been written to implement this curve fitting routine. Apart from the frequency range and the sampling interval which are in general determined by the data at hand, there are three parameters which must be chosen at the outset. They are the orders of the numerator and denominator polynomials, M and N respectively, and the maximum allowed error which terminates the iteration. At the conclusion of the program, the poles and residues of the rational function approximation are computed. The process is then repeated using other (distinct) data for the response of the same body, and those poles which are common to most of the results are identified as SEM poles of the body.

To better understand the limitations of the method and to gain experience in the selection of the parameters involved, it is helpful to consider data for a frequency response whose poles and residues are known precisely. This is true in particular for the surface field on a perfectly conducting sphere.

A sphere of radius a is illuminated by the plane wave

$$\vec{E}^i = \hat{x} e^{i\omega z/c}, \quad \vec{H}^i = -\hat{y} Y e^{i\omega z/c}$$

propagating in the direction of the negative z axis of the Cartesian coordinate system (x,y,z) . Y is the intrinsic admittance of the surrounding free space medium, c is the velocity of light in vacuo, and a time factor $e^{i\omega t}$ has been assumed and suppressed. If (r,θ,ϕ) are spherical polar coordinates, the tangential components of the total magnetic field at the surface $r = a$ are

$$H_\theta = YT_1 \left(\frac{\omega a}{c}, \theta \right) \sin \phi, \quad H_\phi = YT_2 \left(\frac{\omega a}{c}, \theta \right) \cos \phi$$

(Bowman et al., 1969; pp. 396 and 397) with

$$T_1 \left(\frac{\omega a}{c}, \theta \right) = \frac{c}{\omega a} \sum_{n=1}^{\infty} i^{n+1} \frac{2n+1}{n(n+1)} \left\{ \frac{1}{\xi_n^{(2)} \left(\frac{\omega a}{c} \right)} \frac{P_n^{(1)}(\cos \theta)}{\sin \theta} + \frac{i}{\xi_n^{(2)} \left(\frac{\omega a}{c} \right)} \frac{\partial}{\partial \theta} P_n^{(1)}(\cos \theta) \right\} \quad (3a)$$

$$T_2\left(\frac{\omega a}{c}, \theta\right) = \frac{c}{\omega a} \sum_{n=1}^{\infty} i^{n+1} \frac{2n+1}{n(n+1)} \left\{ \frac{1}{\xi_n^{(2)'}\left(\frac{\omega a}{c}\right)} \frac{\partial}{\partial \theta} p_n^{(1)}(\cos \theta) + \frac{i}{\xi_n^{(2)}\left(\frac{\omega a}{c}\right)} \frac{p_n^{(1)}(\cos \theta)}{\sin \theta} \right\} \quad (3b)$$

where $p_n^{(1)}(\cos \theta)$ is the Legendre function of degree n and order unity as defined by Stratton (1941, p. 401) and

$$\xi_n^{(2)}(x) = x h_n^{(2)}(x) \quad , \quad \xi_n^{(2)'}(x) = \frac{d}{dx} \left\{ x h_n^{(2)}(x) \right\}$$

where $h_n^{(2)}(x)$ is the spherical Hankel function of the second kind of order n .

By appropriate truncation of the infinite series representations, it is a simple matter to compute T_1 and T_2 to any desired accuracy. A program was available (Senior, 1975) for the far zone scattered fields of a sphere and this was modified to compute T_1 and T_2 for $\theta = 0(45)180^\circ$ and $0.2 \leq \omega a/c \leq 7.0$ to six decimal accuracy. In the limit as $\omega \rightarrow 0$, $T_1(0, \theta) = -(3/2)\cos \theta$ and $T_2(0, \theta) = -3/2$.

The functions $\xi_n^{(2)}(x)$ and $\xi_n^{(2)'}(x)$ are proportional to polynomials in x of orders n and $n+1$ respectively whose zeros are the SEM poles. In terms of the complex frequency $s = i\omega a/c$, the polynomials have positive real coefficients which ensures that all zeros lie in the left half plane, and those which do not lie on the negative real s axis occur in complex conjugate pairs. As shown, for example, by Martinez et al. (1972), the zeros can be arranged in layers lying successively

further from the imaginary s axis. When ordered from the right, the odd (even) numbered layers are the electric (magnetic) mode resonances produced by the zeros of $\xi_n^{(2)'}(-is)$ and $\xi_n^{(2)}(-is)$ respectively. In general the dominant SEM poles are those in the first ($\ell = 1$) layer, and the n th pole numbered up from the negative real s axis is a zero of $\xi_n^{(2)'}(-is)$.

T_1 and T_2 can be expressed as

$$T_1(-is, \theta) = \sum_{m=1}^{\infty} \frac{R_1^m(\theta)}{s - s_m}, \quad T_2(-is, \theta) = \sum_{m=1}^{\infty} \frac{R_2^m(\theta)}{s - s_m} \quad (4)$$

where the s_m are zeros of either $\xi_n^{(2)'}(-is)$ or $\xi_n^{(2)}(-is)$, and $R_1^m(\theta)$ and $R_2^m(\theta)$ are the residues of T_1 and T_2 respectively at $s = s_m$.

The residues can be found by computing

$$\left. \frac{d}{ds} \left\{ -is \xi_n^{(2)'}(-is) \right\} \right|_{s=s_m}, \quad \left. \frac{d}{ds} \left\{ -is \xi_n^{(2)}(-is) \right\} \right|_{s=s_m}$$

and then dividing these into the quantities

$$i^{n+1} \frac{2n+1}{n(n+1)} F_n(\theta)$$

where $F_n(\theta)$ is either $(\partial/\partial\theta)P_n^{(1)}(\cos\theta)$ or $P_n^{(1)}(\cos\theta)/\sin\theta$. For $\theta = 0$ the poles and residues of the first six poles in the first layer are given in Table 1. For comparison we note that for the first pole (at $s = -1$) in the second layer, $R_1(0) = R_2(0) = -i0.551819$.

Table 1: Exact poles and residues for first layer poles

m	s_m	$R_2^m(0)$
1	$-0.500000 + i0.866025$	$-0.0946447 - i0.516674$
2	$-0.701964 + i1.80740$	$0.633323 - i0.0853256$
3	$-0.842862 + i2.75786$	$0.0802221 + i0.733736$
4	$-0.954230 + i3.71478$	$-0.822075 + i0.0767481$
5	$-1.04764 + i4.67641$	$-0.0741270 - i0.901805$
6	$-1.12891 + i5.64163$	$-0.0664705 + i0.223154$

3. Exact Data Analysis

The curve fitting algorithm was applied to the computed data for T_2 as a function of frequency in an attempt to extract a handful of the lowest order SEM poles. The objective was to locate 4 or 5 pole pairs with sufficient accuracy to leave no doubt as to their identification as SEM (rather than curve fitting) poles, and to allow us to determine the θ dependence of their residues. Data were available for $0.2 \leq \omega a/c \leq 7.0$ in increments of 0.1 and 0.02, and in the expectation that the poles which could be accurately located would be the dominant ones with $\text{Im } s_m$ within the frequency range covered by the data, it was anticipated that most (if not all) poles would lie in the first layer.

To apply the algorithm there are a number of parameters which must be chosen, some of which relate to the data and others to the curve fitting process. Regarding the data, there are the minimum, maximum and increments of $\omega a/c$ and, in our case, the choice of phase reference for the frequency response. Since our concern was with the lower order poles, it was natural to choose $\min \omega a/c$ to be the smallest value for which data was available, namely 0.2; and to avoid handling more data than was clearly necessary, we initially selected $\max \omega a/c = 4.0$ with increments of 0.1. The computed data of Section 2 are phase-referenced to a plane perpendicular to the z axis through the center of the sphere. For all θ except $\pi/2$, $\arg T_2$ varies almost linearly as a function of frequency, and this translates into a roughly sinusoidal variation of the real and imaginary parts which are the inputs to the curve fitting process. The variation is greatly reduced

if the phase is referenced to the point on the surface of the sphere where the field is computed, and since it is natural to expect that a smooth curve can be fitted more accurately than a rapidly varying one, $\arg T_2$ was increased by $\omega a/c \cos \theta$ prior to the application of the algorithm. Once the curve fitting was accomplished and the poles and residues determined, the phase reference was returned to the original location.

Three parameters involved in the program itself are the orders M and N of the numerator and denominator polynomials and the maximum allowed error E_{\max} . Since the set of SEM poles is infinite in number and the response remains finite as $\omega a/c \rightarrow \infty$, it would seem that the accuracy of curve fit should increase with M and N, and that a logical choice would be $M = N$. Numerically, however, problems are experienced when M and/or N are large due to the finite range of numbers that any computer can handle, whereas if N is small there are too few poles available to simulate the data. It was therefore anticipated that there would be an optimum range of N and, perhaps, M depending on the frequency span of the data and the particular characteristics of the computer.

The error E_{\max} relates to the convergence of the iterative process and is not directly a measure of the curve fit nor, of course, the accuracy of pole extraction. When running the program, E_{\max} was set at 10^{-8} and the iteration was terminated when this value was achieved, or after 20 iterations, whichever came first. In many instances the maximum allowed error was not obtained, but the curve fit was still excellent. As a measure of the curve fit we therefore computed

$$E_{\text{fit}} = \frac{1}{L} \sum_{\ell=1}^L \left| F(\omega_{\ell}) - \frac{N_k(\omega_{\ell})}{D_k(\omega_{\ell})} \right|^2 \quad (5)$$

(c.f. (2)), where the polynomials are those obtained from the final iteration, and recorded this quantity. Due to the limited precision with which the data were stored, any value of E_{fit} less than 0.25×10^{-7} was shown to be zero. Since the curve fit was excellent in most cases, it was not unusual for this to occur.

All of the initial runs were carried out for $\theta = 0$ (for which $T_2 = T_1$). It was found almost immediately that numerical difficulties arise if N exceeds (about) 25, and if $M = N$, these problems can occur for M, N as small as 18. In either instance the exponential range of the computer (Amdahl 470/V8) was exceeded. We therefore chose $M < N$, and because of the restriction on N , limited the frequency span of the data to $\omega a/c \leq 4.0$ to allow for a reasonable number of curve fitting poles in addition to the SEM poles that were sought.

Figure 1 shows the curve fit to $|F(\omega_{\ell})|$ for $\theta = 0$ and $\Delta\omega a/c = 0.1$ with $M = 7$ and $N = 8$. The criterion for E_{max} was met and $E_{\text{fit}} = 0.25 \times 10^{-3}$. The extracted pole locations are shown in Fig. 2, and we observe that three of the poles vaguely resemble the first three SEM poles, more closely as regards $\text{Im } s_m$ than $\text{Re } s_m$. The agreement is better if $M = 9$ and $N = 10$, and better still if M and N are increased to 11 and 12 respectively (see Fig. 3). We are now beginning to pick up the fifth SEM pole of the first layer (which lies outside the range of $\text{Im } s$ spanned by the data), as well as the first pole of the second layer. The convergence criterion was again met and

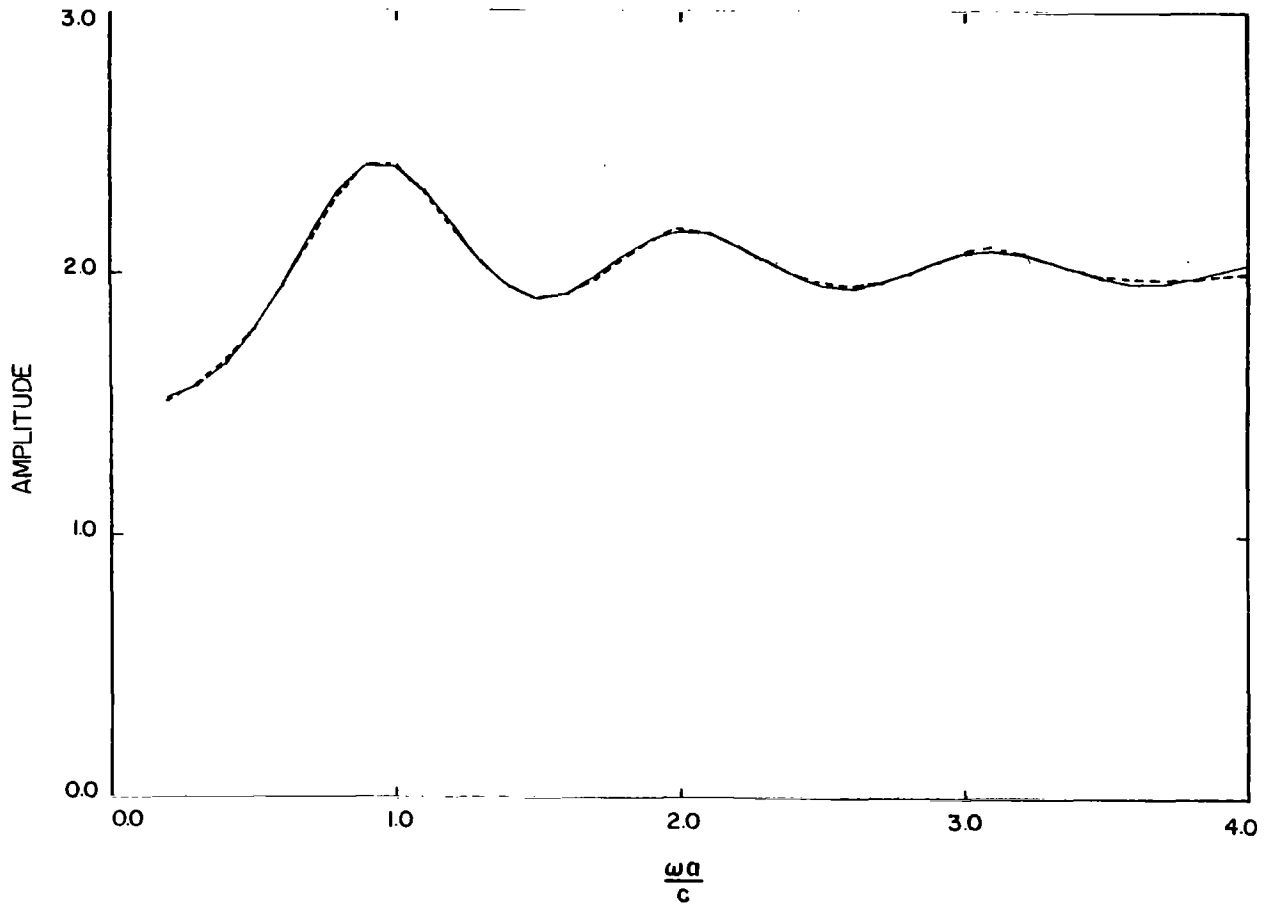


Fig. 1: Comparison of $T_2(0)$ (—) and the curve fit (---) obtained with $\omega a/c = 0.2(0.1)4.0$, $M = 7$ and $N = 8$.

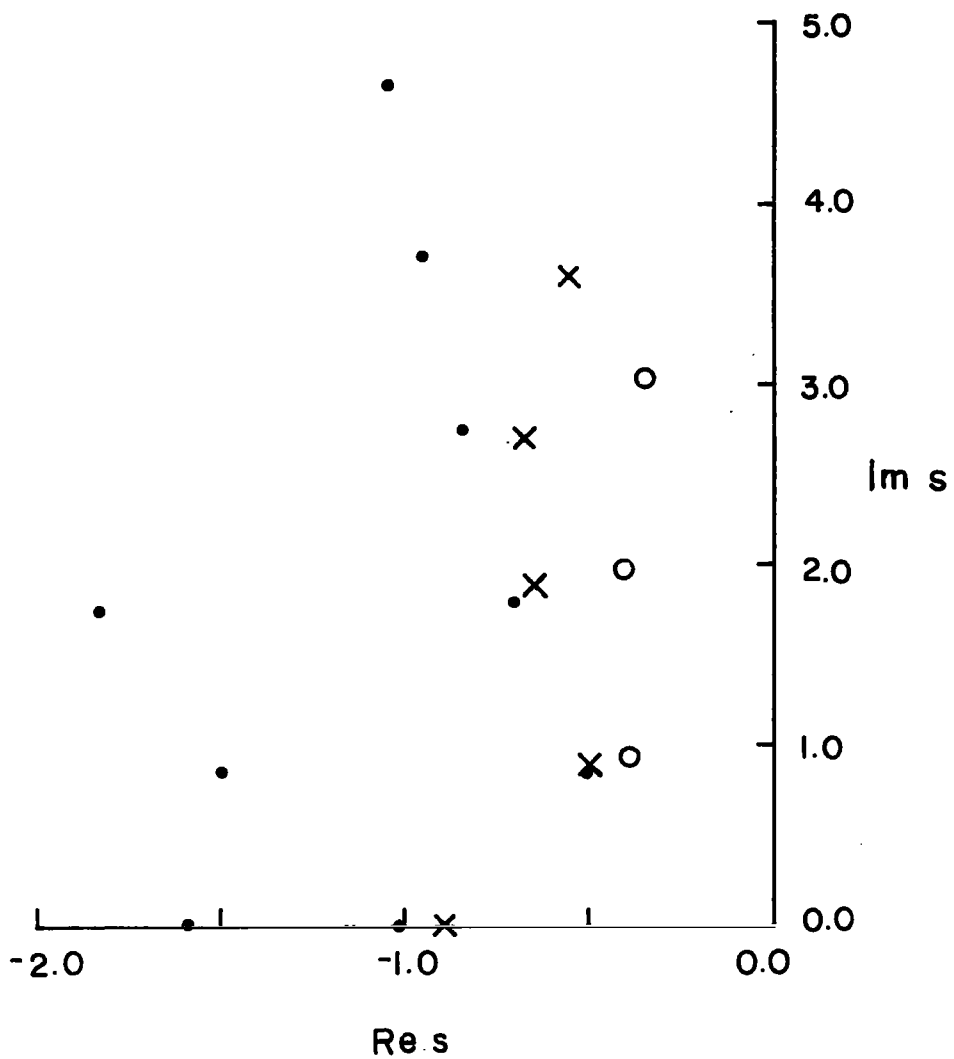


Fig. 2: Comparison of exact (••) and fitted function poles for $M = 7$ and $N = 8$ (○ ○) and for $M = 9$ and $N = 10$ (× ×).

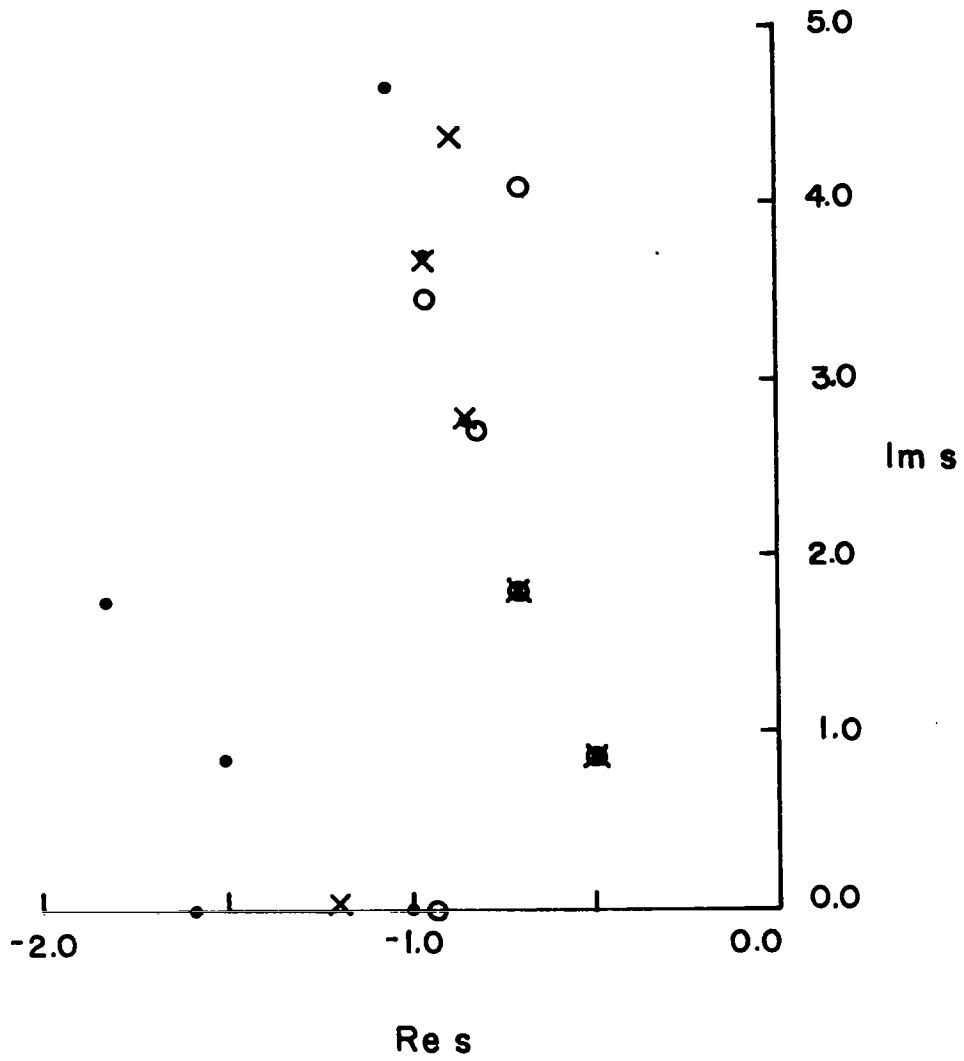


Fig. 3: Comparison of exact (• •) and fitted function poles for $M = 11$ and $N = 12$ (○ ○) and for $M = 15$ and $N = 16$ (× ×).

$E_{fit} = 0.51 \times 10^{-7}$. In this case and in all others discussed, the modulus of the simulated response was graphically indistinguishable from the data within the frequency range spanned by the data, but as seen from Fig. 4, there are discrepancies outside the range.

Table 2 compares the locations of the first four SEM poles with those of the extracted poles for $\theta = 0$, $\Delta\omega a/c = 0.1$ and four M and N combinations. In each case $E_{fit} \approx 0$ and the agreement in pole locations improves with increasing order of the polynomials. The best results are for M = 15 and N = 16 in the sense that a further increase in M and/or N gives no improvement. Similar comparisons for a variety of polynomial orders from 8 to 18 have shown that the accuracy of the extracted poles is best for M = N-1 and diminishes for N \geq 20.

For given M and N a decrease in the sampling interval from 0.1 (39 data points) to 0.02 (191 data points) has no appreciable effect, as indicated in Table 3. The results of shifting the phase reference of the data to a plane through the center of the sphere are shown in Table 4 and, as expected, the accuracy of the pole locations is poorer.

The above data are all for $\theta = 0$, and for the cases considered in Tables 2 through 4 the accuracy of curve fit is extremely good. However, this does not imply a comparable accuracy in the extracted pole locations, and in a practical situation where the locations of the true poles are unknown, it is necessary to vary the illumination conditions, e.g., change θ , and use the positional invariance of the true poles as the criterion of accuracy. We also comment that E_{fit} is unrelated to E_{max} , and for the cases in Tables 2 through 4, the specified error 10^{-8} was never achieved prior to the completion of the allowed 20 iterations.

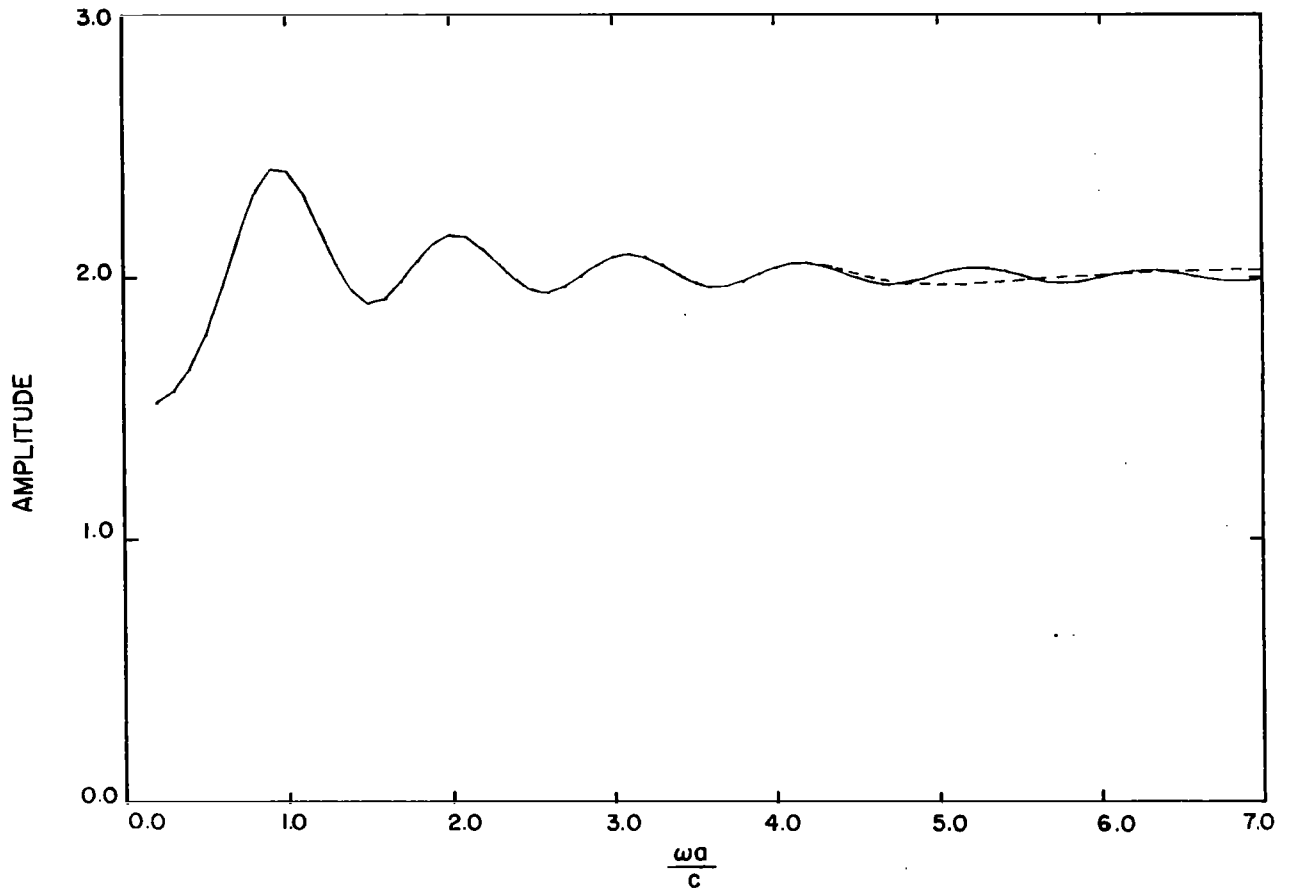


Fig. 4: Comparison of $T_2(0)$ (—) and the curve fit (---) obtained with $\omega a/c = 0.2(0.1)4.0$, $M = 11$ and $N = 12$.

Table 2: Comparison of exact and extracted pole locations for $\theta = 0$,
 $\Delta\omega a/c = 0.1$ and various M, N

Exact	Extracted			
	M=12, N=14	M=13, N=14	M=14, N=16	M=15, N=16
-0.500000	-0.5010	-0.5007	-0.5007	-0.5000
$\pm i0.866025$	$\pm i0.8641$	$\pm i0.8659$	$\pm i0.8657$	$\pm i0.8658$
-0.701964	-0.6964	-0.7052	-0.7027	-0.7025
$\pm i1.80740$	$\pm i1.808$	$\pm i1.804$	$\pm i1.803$	$\pm i1.806$
-0.842862	-0.8436	-0.8334	-0.8408	-0.8399
$\pm i2.75786$	$\pm i2.739$	$\pm i2.762$	$\pm i2.766$	$\pm i2.760$
-0.954230	-1.056	-0.9309	-0.9199	-0.9439
$\pm i3.71478$	$\pm i3.575$	$\pm i3.642$	$\pm i3.685$	$\pm i3.678$

Table 3: Comparison of exact and extracted pole locations for $\theta = 0$,
 showing the effect of $\Delta\omega a/c$

Exact	Extracted			
	M = 13, N = 14		M = 15, N = 16	
	$\Delta\omega a/c = 0.02$	$\Delta\omega a/c = 0.1$	$\Delta\omega a/c = 0.02$	$\Delta\omega a/c = 0.1$
-0.500000 $\pm i0.866025$	-0.5003 $\pm i0.8635$	-0.5007 $\pm i0.8659$	-0.4999 $\pm i0.8657$	-0.5000 $\pm i0.8658$
-0.701964 $\pm i1.80740$	-0.6997 $\pm i1.810$	-0.7052 $\pm i1.804$	-0.7021 $\pm i1.806$	-0.7025 $\pm i1.806$
-0.842862 $\pm i2.75786$	-0.8364 $\pm i2.752$	-0.8334 $\pm i2.762$	-0.8407 $\pm i2.760$	-0.8399 $\pm i2.760$
-0.954230 $\pm i3.71478$	-0.9721 $\pm i3.647$	-0.9309 $\pm i3.642$	-0.9489 $\pm i3.682$	-0.9439 $\pm i3.678$

Table 4: Comparison of exact and extracted pole locations for $\theta = 0$
and $\Delta\omega a/c = 0.1$, showing the effect of phase reference

Exact	Extracted			
	M = 13, N = 14		M = 15, N = 16	
	center	surface	center	surface
-0.500000	-0.5010	-0.5007	-0.5009	-0.5000
$\pm i0.866025$	$\pm i0.8655$	$\pm i0.8659$	$\pm i0.8650$	$\pm i0.8658$
-0.701964	-0.6994	-0.7052	-0.6994	-0.7025
$\pm i1.80740$	$\pm i1.801$	$\pm i1.804$	$\pm i1.804$	$\pm i1.806$
-0.842862	-0.8600	-0.8334	-0.8522	-0.8399
$\pm i2.75786$	$\pm i2.770$	$\pm i2.762$	$\pm i2.769$	$\pm i2.760$
-0.954230	-0.8879	-0.9309	-0.8794	-0.9439
$\pm i3.71478$	$\pm i3.797$	$\pm i3.642$	$\pm i3.785$	$\pm i3.678$

The effect of changing θ is shown in Table 5, which gives the extracted pole locations for $\theta = 0(45)180^\circ$ with $M = 15$, $N = 16$ and $\Delta\omega a/c = 0.1$. The accuracy does not vary significantly with θ , though we observe that at $\theta = 90^\circ$ where the first and third poles are not excited, the accuracy of the second and fourth poles is better than before. The residues $R_2^m(\theta)$ of the first four poles for T_2 are plotted in Figs. 5 through 8, and the somewhat poorer accuracy with which the fourth pole is located, particularly for $\theta > 90^\circ$, is reflected in its residue.

The fourth pole is fairly close to the upper limit of the frequencies spanned by the data. To improve its accuracy and, at the same time, locate the next pole or two, it is natural to increase $\max \omega a/c$ to 5 or 6, and the results of doing so are shown in Table 6. The best agreement is obtained with $M = 17$ and $N = 18$. Although the curve fit is again excellent, as it was for $M = 15$ and $N = 16$ with the smaller data set (see Table 3), the first three poles are not quite as accurately located, but the fourth through sixth are in reasonable agreement. Unfortunately, to increase the data span still more and extract further poles requires the use of polynomials of higher order, and because of the numerical difficulties that occur when N exceeds (about) 25, this does not prove to be effective. An alternative approach is to retain the same span of data and 'window', i.e., shift the span to encompass those poles which are sought. This is illustrated in Table 7 for three different M and N combinations applied to the data for $2.0 \leq \omega a/c \leq 6.0$. In terms of the accuracy of the extracted poles, the case $M = 15$ and $N = 16$ is best. The fourth through sixth poles are located more accurately than with the larger frequency span, but the first pole is

Table 5: Comparison of exact and extracted pole locations for $\Delta\omega a/c = 0.1$,
 $M = 15$, $N = 16$ and $\theta = 0(45)180^\circ$

Exact	Extracted				
	$\theta = 0^\circ$	$\theta = 45^\circ$	$\theta = 90^\circ$	$\theta = 135^\circ$	$\theta = 180^\circ$
-0.500000 $\pm i0.866025$	-0.5000 $\pm i0.8658$	-0.5000 $\pm i0.8661$	not excited	-0.4997 $\pm i0.8661$	-0.5001 $\pm i0.8660$
-0.701964 $\pm i1.80740$	-0.7025 $\pm i1.806$	not excited	-0.7020 $\pm i1.807$	not excited	-0.7008 $\pm i1.808$
-0.842862 $\pm i2.75786$	-0.8399 $\pm i2.760$	-0.8418 $\pm i2.760$	not excited	-0.8419 $\pm i2.759$	-0.8410 $\pm i2.751$
-0.954230 $\pm i3.71478$	-0.9439 $\pm i3.678$	-0.9490 $\pm i3.698$	-0.9565 $\pm i3.716$	-0.9341 $\pm i3.732$	-0.9310 $\pm i3.622$

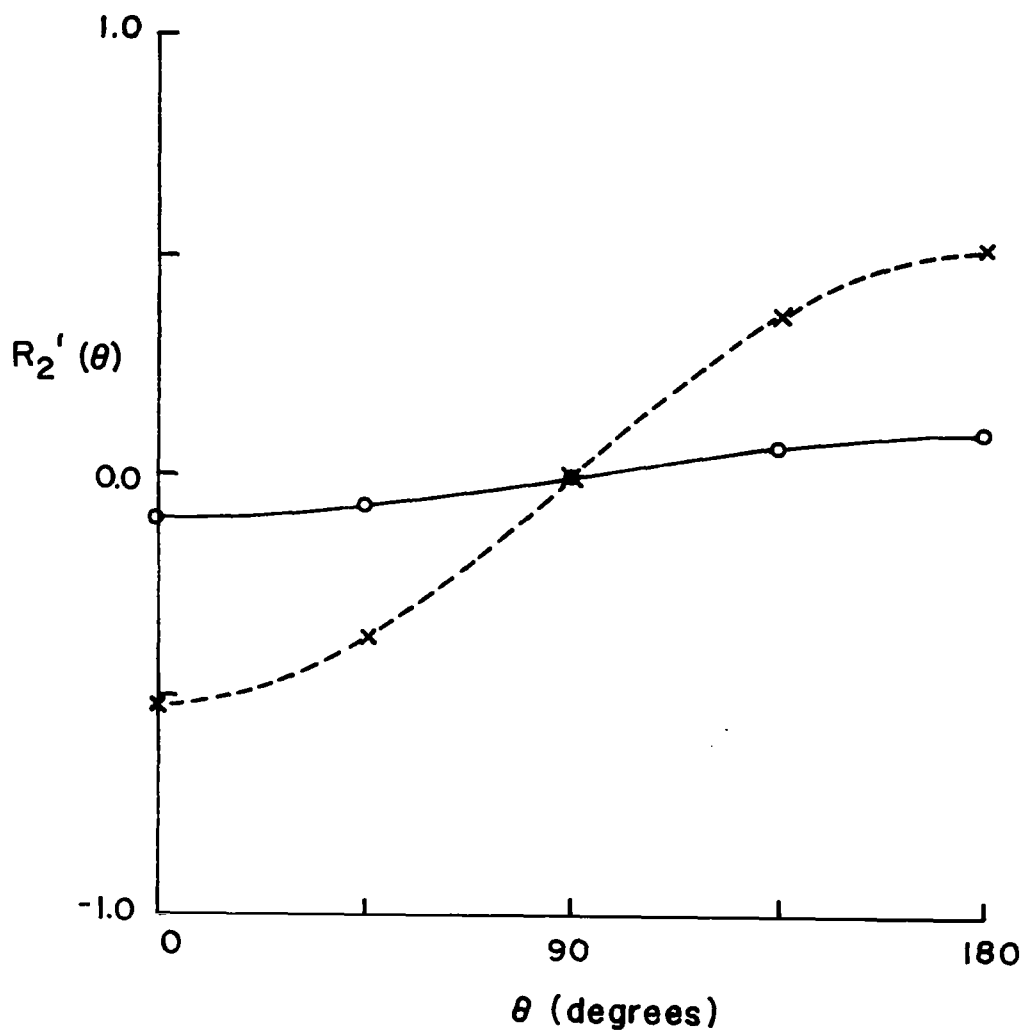


Fig. 5: Real (—) and imaginary (---) parts of the residue, $R_2'(\theta)$, of the first pole for the first layer and the extracted real (O O) and imaginary (X X) parts.

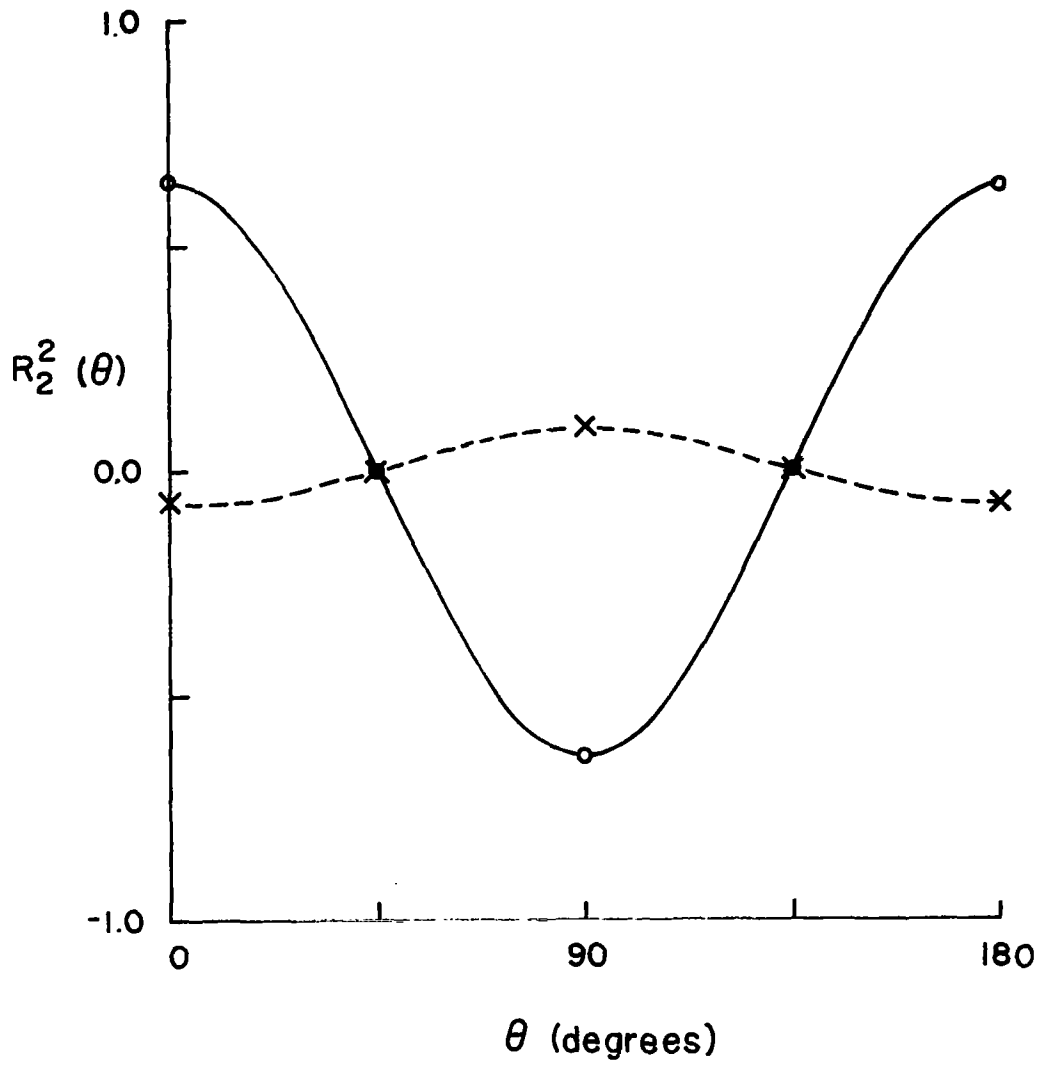


Fig. 6: Real (—) and imaginary (---) parts of the residue, $R_2^2(\theta)$, of the second pole of the first layer and the extracted real (O O) and imaginary (X X) parts.

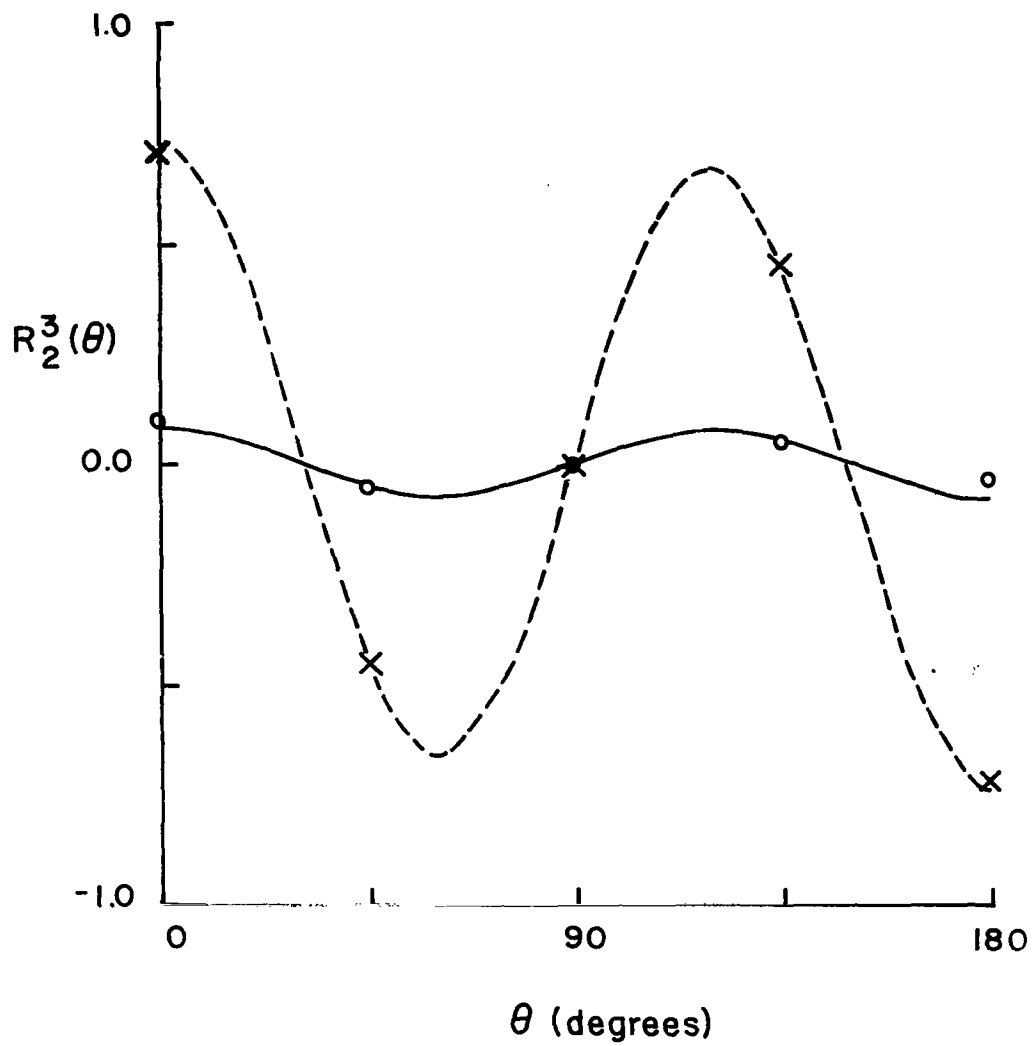


Fig. 7: Real (—) and imaginary (---) parts of the residue, $R_2^3(\theta)$, of the third pole of the first layer and the extracted real ($\circ \circ$) and imaginary ($\times \times$) parts.

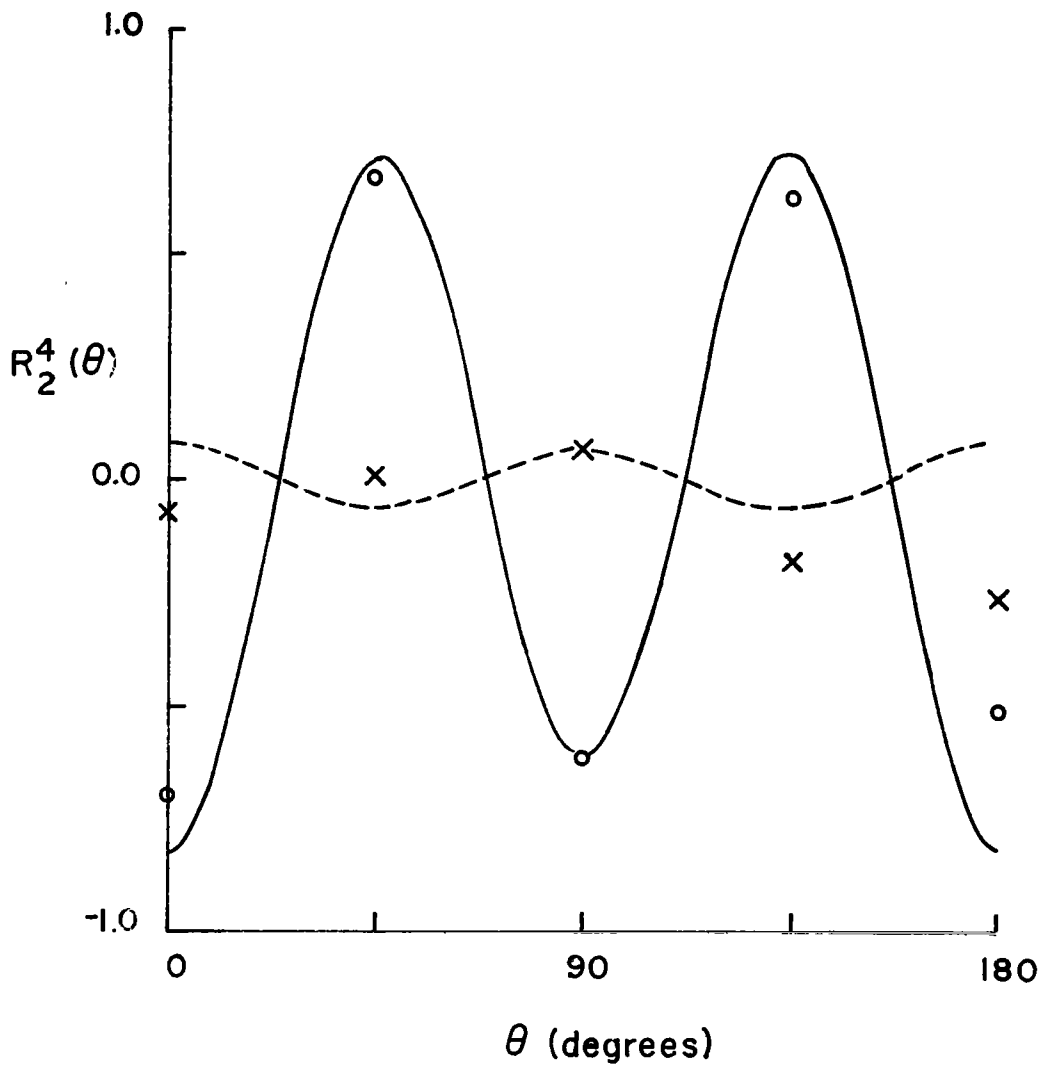


Fig. 8: Real (—) and imaginary (---) parts of the residue, $R_2^4(\theta)$, of the fourth pole of the first layer and the extracted real (\circ) and imaginary (\times) parts.

Table 6: Comparison of exact and extracted pole locations for
 $\theta = 0$, and $\omega a/c = 0.2(0.1)6.0$

Exact	Extracted		
	M = 15, N = 16	M = 17, N = 18	M = 19, N = 20
-0.500000	-0.5020	-0.5007	-0.5008
$\pm i0.866025$	$\pm i0.8643$	$\pm i0.8637$	$\pm i0.8638$
-0.701964	-0.6935	-0.6986	-0.6980
$\pm i1.80740$	$\pm i1.812$	$\pm i1.810$	$\pm i1.809$
-0.842862	-0.8252	-0.8370	-0.8369
$\pm i2.75786$	$\pm i2.742$	$\pm i2.753$	$\pm i2.751$
-0.954230	-0.9472	-0.9532	-0.9567
$\pm i3.71478$	$\pm i3.649$	$\pm i3.697$	$\pm i3.693$
-1.04764	-1.061	-1.073	-1.090
$\pm i4.67641$	$\pm i4.464$	$\pm i4.622$	$\pm i4.619$
-1.12891	-0.9781	-1.161	-0.8810
$\pm i5.64163$	$\pm i5.183$	$\pm i5.372$	$\pm i6.046$

Table 7: Comparison of exact and extracted pole locations for
 $\theta = 0$, and $\omega a/c = 2.0(0.1)6.0$

Exact	Extracted		
	M = 15, N = 16	M = 17, N = 18	M = 19, N = 20
-0.500000 $\pm i0.866025$	not located	not located	not located
-0.701964 $\pm i1.80740$	-0.6365 $\pm i1.802$	-0.7005 $\pm i1.730$	-0.6025 $\pm i1.816$
-0.842862 $\pm i2.75786$	-0.8449 $\pm i2.746$	-0.8558 $\pm i2.765$	-0.8536 $\pm i2.730$
-0.954230 $\pm i3.71478$	-0.9582 $\pm i3.714$	-0.9422 $\pm i3.728$	-0.9787 $\pm i3.738$
-1.04764 $\pm i4.67641$	-1.041 $\pm i4.656$	-1.011 $\pm i4.658$	-1.011 $\pm i4.728$
-1.12891 $\pm i5.64163$	-1.079 $\pm i5.467$	-1.054 $\pm i5.497$	-0.9399 $\pm i5.658$

not picked up at all, and the second is considerably in error. This is hardly surprising since the first two poles are no longer spanned by the data.

As a result of the above investigation, the following conclusions can be drawn. In the first place, the data should fully span the imaginary parts of the poles to be located. If n SEM poles are spanned, N should be in the range $3n$ to $4n$ with $M = N-1$, but N should not exceed (about) 25 to avoid numerical difficulties. This upper limit decreases with increasing $\max \omega a/c$ and is almost certainly machine dependent as well. For a greater span of data and/or to extract more than a handful of SEM poles, it may be necessary to process the data in batches (perhaps overlapping), i.e., use windowing.

4. Effect of Noise

In most practical applications of the pole extraction method, the data for the frequency response have been obtained by measurement or by the numerical solution of a less than perfect model of the scatterer. Inevitably such data are subject to noise and other uncertainties, and it is important to see how the accuracy of both the curve fit and the SEM pole extraction are affected. For this purpose, two types of noise were considered: numerical inaccuracies in the form of data limited to k decimal places, and added Gaussian white noise of various amplitudes.

For the first study, the real and imaginary parts of $T_2(0)$ which were originally accurate to six decimal places were rounded to k decimals with k progressively reduced. The data used spanned $0.2 \leq \omega a/c \leq 4.0$ in increments of 0.1 and 0.02, and since a rational

function with $M = 15$ and $N = 16$ had proved to be effective in the absence of noise (i.e., when $k = 6$), this function was chosen. For $\Delta\omega a/c = 0.1$ and 0.02 the curve fits were equally good, but because the accuracy of the extracted poles was slightly better for the closer sampling, we used this in all of the noise studies.

As k was reduced down to 1, the extracted poles became increasingly inaccurate as shown in Table 8, and for $k = 2$ even the dominant pole was substantially in error. In spite of this, the curve fit remained good. Figure 9 shows the loci of the extracted poles as functions of k . As k decreases, each pole moves closer to the imaginary s axis, and the general behavior is similar to that found when fitting the exact data with rational functions of progressively lower order. This suggests that by increasing M and N we might be able to overcome some of the noise effects and thereby improve the accuracy of the extracted poles. Because of the numerical difficulties referred to earlier, the largest N that could easily be handled was 24, and the results of using $M = 23$ and $N = 24$ with data having $k = 3$ and 2 are presented in Table 9. The increased order of polynomials produces only a slight improvement, primarily for the data with $k = 2$.

In the second study Gaussian distributed white noise was added to the exact data for the real and imaginary parts of $T_2(0)$, $\omega a/c = 0.2(0.02)4.0$. The noise was produced by a random number generator for which the mean and standard deviation could be specified. In all cases the mean was chosen to be zero and the standard deviation varied to change the noise level. For noise with standard deviations 10^{-5} and 10^{-4} , the values of E_{fit} and the pole locations provided by a

Table 8: Comparison of exact and extracted poles for $\theta = 0$, $\omega a/c = 0.2(0.02)4.0$,
 $M = 15$ and $N = 16$, with data sets rounded to k decimal places

Exact	Extracted				
	k = 6	k = 4	k = 3	k = 2	k = 1
-0.500000 $\pm i0.866025$	-0.5000 $\pm i0.8658$	-0.5011 $\pm i0.8639$	-0.5140 $\pm i0.8577$	-0.4081 $\pm i0.8369$	-0.3764 $\pm i0.9174$
-0.701964 $\pm i1.80740$	-0.7025 $\pm i1.806$	-0.6957 $\pm i1.811$	-0.7005 $\pm i1.861$	-0.4924 $\pm i1.643$	-0.2961 $\pm i1.939$
-0.842862 $\pm i2.75786$	-0.8399 $\pm i2.760$	-0.8323 $\pm i2.732$	-0.7548 $\pm i2.842$	-0.4727 $\pm i2.516$	-0.1581 $\pm i2.964$
-0.954230 $\pm i3.71478$	-0.9439 $\pm i3.678$	-0.9614 $\pm i3.517$	-0.6875 $\pm i3.784$	-0.3981 $\pm i3.924$	-0.04094 $\pm i3.257$
E_{fit}	$<0.25 \times 10^{-7}$	0.27×10^{-1}	0.27×10^{-1}	0.27×10^{-1}	0.31×10^{-1}

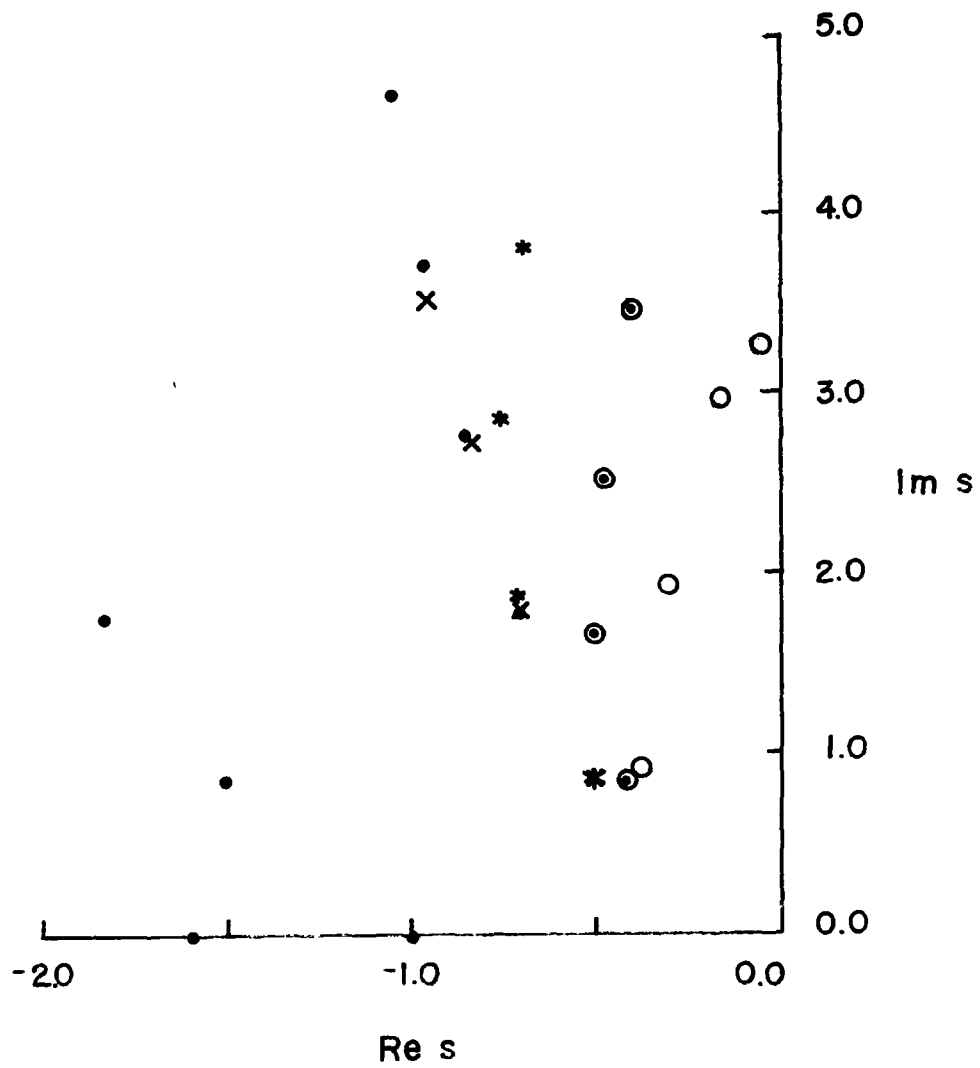


Fig. 9: Comparison of exact ($\bullet\bullet$) and extracted poles for $\theta = 0$, $\omega a/c = 0.2(0.1)4.0$, $M = 15$ and $N = 16$ with data rounded to $k = 1$ ($\circ\circ$), $k = 2$ ($\odot\odot$), $k = 3$ ($*\ast$), and $k = 4$ ($\times\times$) decimal places.

Table 9: Comparison of exact and extracted pole locations for $\theta = 0$,
and $\omega a/c = 0.2(0.02)4.0$ for various decimal places k of
data accuracy

Exact	Extracted			
	k = 3		k = 2	
	M = 15, N = 16	M = 23, N = 24	M = 15, N = 16	M = 23, N = 24
-0.500000 $\pm i0.866025$	-0.5140 $\pm i0.8577$	-0.5054 $\pm i0.8648$	-0.4081 $\pm i0.8369$	-0.4824 $\pm i0.8051$
-0.701964 $\pm i1.80740$	-0.7005 $\pm i1.861$	-0.6873 $\pm i1.827$	-0.4924 $\pm i1.643$	-0.6564 $\pm i1.676$
-0.842862 $\pm i2.75786$	-0.7548 $\pm i2.842$	-0.7488 $\pm i2.753$	-0.4727 $\pm i2.516$	-0.6578 $\pm i2.643$
-0.954230 $\pm i3.71478$	-0.6875 $\pm i3.784$	-0.6607 $\pm i3.670$	-0.3981 $\pm i3.924$	-0.5721 $\pm i3.620$
E_{fit}	0.27×10^{-1}	0.27×10^{-1}	0.27×10^{-1}	0.27×10^{-1}

rational function having $M = 15$ and $N = 16$ are listed in Table 10, and even in the former case, the extracted poles differ substantially from the exact ones. Figure 10 shows the curve fit to the magnitudes of the noisy data for the standard deviation 10^{-4} .

As a final test the curve fitting and pole extraction algorithm was applied to measured data for the field component T_2 at the front ($\theta = 0$) of a metallic sphere 6 inches in diameter (Fig. 11). The data were obtained in an anechoic chamber over the frequency range 0.118 to 4.4 GHz, corresponding to $0.2 \leq \omega a/c \leq 7.0$, but only the data for $0.2 \leq \omega a/c \leq 4.0$ were used. Since prior studies using measured data for the fields at the surface of a thick cylinder had shown that filtering could remove some of the experimental noise, the measured data were also processed using a seventh order digital filter. For both the unfiltered and filtered data, the results of pole extraction with a rational function having $M = 15$ and $N = 16$ are given in Table 11, and are comparable to those in Table 10 for Gaussian noise with standard deviations 10^{-4} and 10^{-5} respectively. Although filtering gives some slight improvement in the accuracy with which the second, third and fourth poles are located, it does so at the expense of a decrease in the accuracy of the first pole.

As a result of these studies it appears unlikely that the curve fitting and pole extraction algorithm can accurately locate more than (at most) the first (dominant) SEM pole using measured data for the frequency response.

Table 10: Comparison of exact and extracted pole locations for $\theta = 0$, $\omega a/c = 0.2(0.02)4.0$, $M = 15$ and $N = 16$ for different levels of Gaussian distributed white noise

Exact	Extracted	
	std. dev. = 10^{-5}	std. dev. = 10^{-4}
-0.500000 $\pm i0.866025$	-0.4492 $\pm i0.8313$	-0.3907 $\pm i0.9026$
-0.701964 $\pm i1.80740$	-0.6022 $\pm i1.700$	-0.4235 $\pm i1.855$
-0.842862 $\pm i2.75786$	-0.5819 $\pm i2.625$	-0.3092 $\pm i2.849$
-0.954230 $\pm i3.71478$	-0.4773 $\pm i3.582$	-0.06515 $\pm i3.436$
E_{fit}	0.27×10^{-4}	0.38×10^{-3}

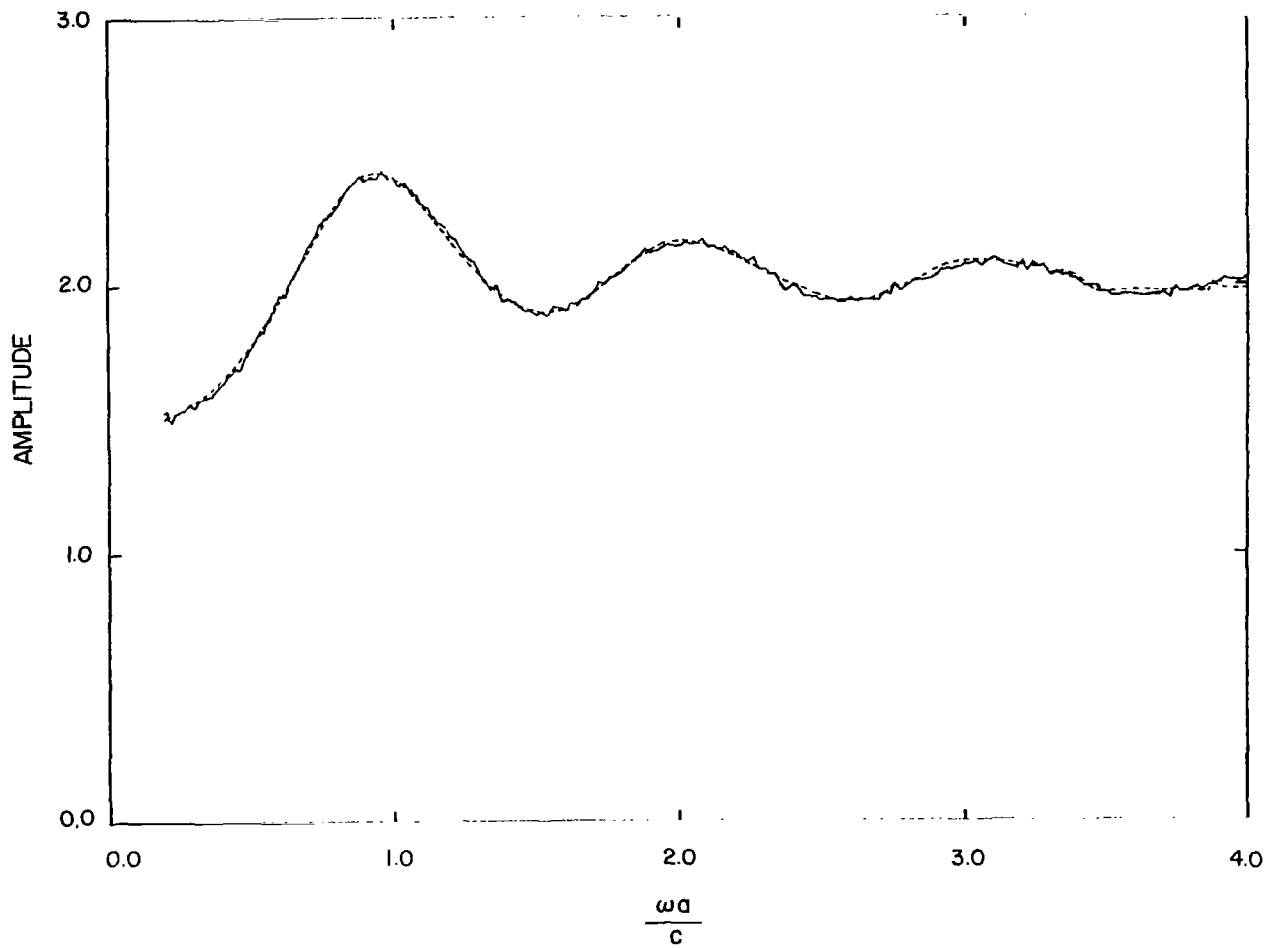


Fig. 10: Comparison of $T_2(0)$ with additive noise level of std. dev. = 10^{-4} (—) and the curve fit (---) obtained with $\omega a/c = 0.2(0.02)4.0$, $M = 15$ and $N = 16$.

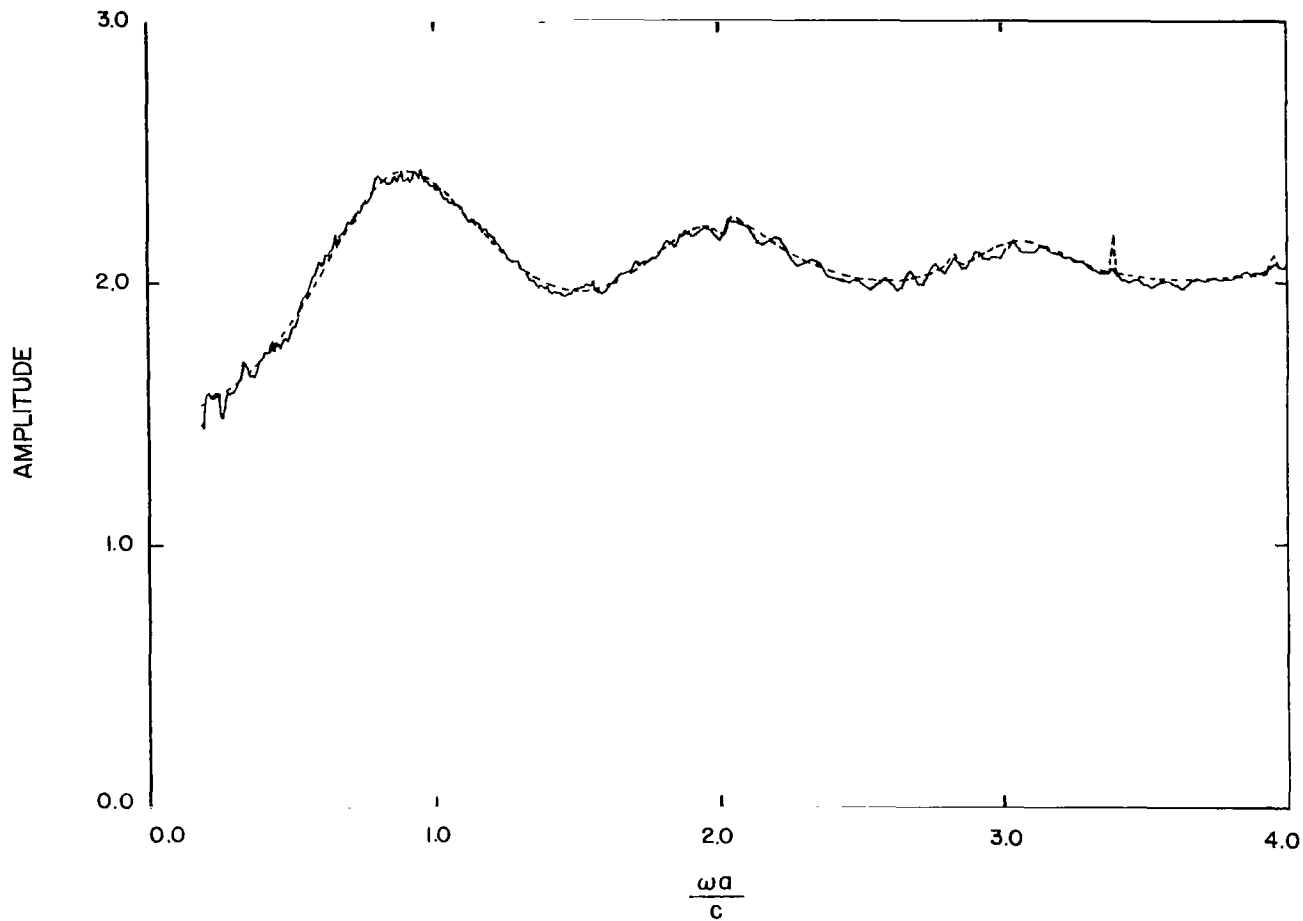


Fig. 11: Comparison of experimental data at $\theta = 0$ (—) and the curve fit (---) obtained with $0.2 \leq \omega a/c \leq 4.0$, $M = 15$ and $N = 16$.

Table 11: Comparison of exact and extracted pole locations for measured data at $\theta = 0$ with $0.2 \leq \omega a/c \leq 4.0$, $M = 15$ and $N = 16$

Exact	Extracted	
	Experimental	Filtered Experimental
-0.500000 $\pm i0.866025$	-0.3920 $\pm i0.8575$	-0.3709 $\pm i0.8014$
-0.701964 $\pm i1.80740$	-0.3530 $\pm i1.927$	-0.4101 $\pm i1.872$
-0.842862 $\pm i2.75786$	-0.2764 $\pm i3.066$	-0.4258 $\pm i2.662$
-0.954230 $\pm i3.71478$	not located	-0.3332 $\pm i3.764$
E_{fit}	0.77×10^{-1}	0.78×10^{-1}

5. Conclusions

Using rational functions a curve fitting and pole extraction algorithm has been developed and applied to exact frequency domain data for the surface fields on a sphere. The data are fitted extremely closely and for at least a handful of the lowest order SEM poles, the extracted poles and their residues are in good agreement with their known values. It is possible that the method could be further refined to yield a few more poles, but the performance is already close to the limits of the computer. Overall, the success is comparable to that achieved by Brittingham et al (1980) using a frequency domain Prony's method.

Unfortunately, the situation is very different if the frequency response is noisy or degraded in accuracy in a manner typical of measured data. Although the curve fit is still good, even a small amount of noise is sufficient to produce considerable discrepancies between the extracted and true (SEM) poles, and for noise levels characteristic of the best experimental data, it is impossible to locate more than (at most) the dominant SEM pole to any degree of accuracy.

Since these conclusions have been reached using only a single algorithm applied to the frequency response of a sphere alone, it cannot be inferred that all frequency domain methods will be equally affected by noise. Nevertheless, the algorithm is a reasonably sophisticated one and is highly successful in curve fitting the data. Likewise the sphere, though a less resonant structure than (say) a thin wire, has a frequency response which is not unlike that of more complicated targets such as an aircraft. For these reasons, it is probable that the conclusions have general validity.

References

- Baum, C. E. (1976), "The singularity expansion method," in Transient Electromagnetic Fields (ed. L. B. Felsen), Springer-Verlag, Berlin.
- Bowman, J. J., T.B.A. Senior and P.L.E. Uslenghi (1969), "Electromagnetic and acoustic scattering by simple shapes," North-Holland Pub. Co., Amsterdam.
- Brittingham, J. N., E. K. Miller and J. L. Willows (1980), "Pole extraction from real-frequency information," Proc. IEEE 68, No. 2, 263-273.
- Cho, K. S., and J. T. Cordaro (1980), "Calculation of the SEM parameters from the transient response of a thin wire," IEEE Trans. Antennas Propagat. AP-28, No. 6, 921-924, also Interaction Note 379, Sep 79.
- Levy, E. C. (1959), "Complex curve fitting," IRE Trans. Automatic Control AC-4, 37-44.
- Martinez, J. P., Z. L. Pine and F. M. Tesche (1972), "Numerical results of the singularity expansion method as applied to a plane wave incident on a perfectly conducting sphere," Interaction Note 112, May 72
- Sancer, M. I., and A. D. Varvatsis (1980), "Toward an increased understanding of the singularity expansion method," Interaction Note 398, May 1980
- Senior, T.B.A. (1975), "Far field bistatic scattering by a sphere," The University of Michigan Radiation Laboratory Report No. 013741-1-F.
- Sharpe, C. B., and C. J. Roussi (1979), "Equivalent circuit representation of radiation systems," Interaction Note 361, April 79.

Stratton, J. A. (1941), "Electromagnetic theory," McGraw-Hill Book Co.
Inc., New York.